Supporting Information

PVP derived nitrogen-doped porous carbon integrated with polyindole: nano/microspheres assembled by emulsion polymerization for asymmetric supercapacitors

Pengcheng Zhou[a,1] Feng Xiao[a,1] Ruixue Weng[a] Quanguo Huang[a] Lei Wang[a] Qihang He[a] Weishan Tang[a] Peilin Yang[a] Rong Su[a,b] Ping He[a,c*] Bin Jia[c,d] Liang Bian[e]

a School of Materials Science and Engineering, Southwest University of Science and Technology, Mianyang 621010, PR China

b School of Science, Xichang College, Xichang 615013, PR China

c International Science and Technology Cooperation Laboratory of Micro-Nanoparticle Application Research, Mianyang 621010, PR China

d Key Laboratory of Shock and Vibration of Engineering Materials and Structures of Sichuan Province, Southwest University of Science and Technology, Mianyang 621010, PR China

e Key Laboratory of Solid Waste Treatment and Resource Recycle, Southwest University of Science and Technology, Mianyang, 621010, PR China

[1] These authors contributed equally to this work.
[*] Corresponding author. E-mail: heping@swust.edu.cn

Supporting Information

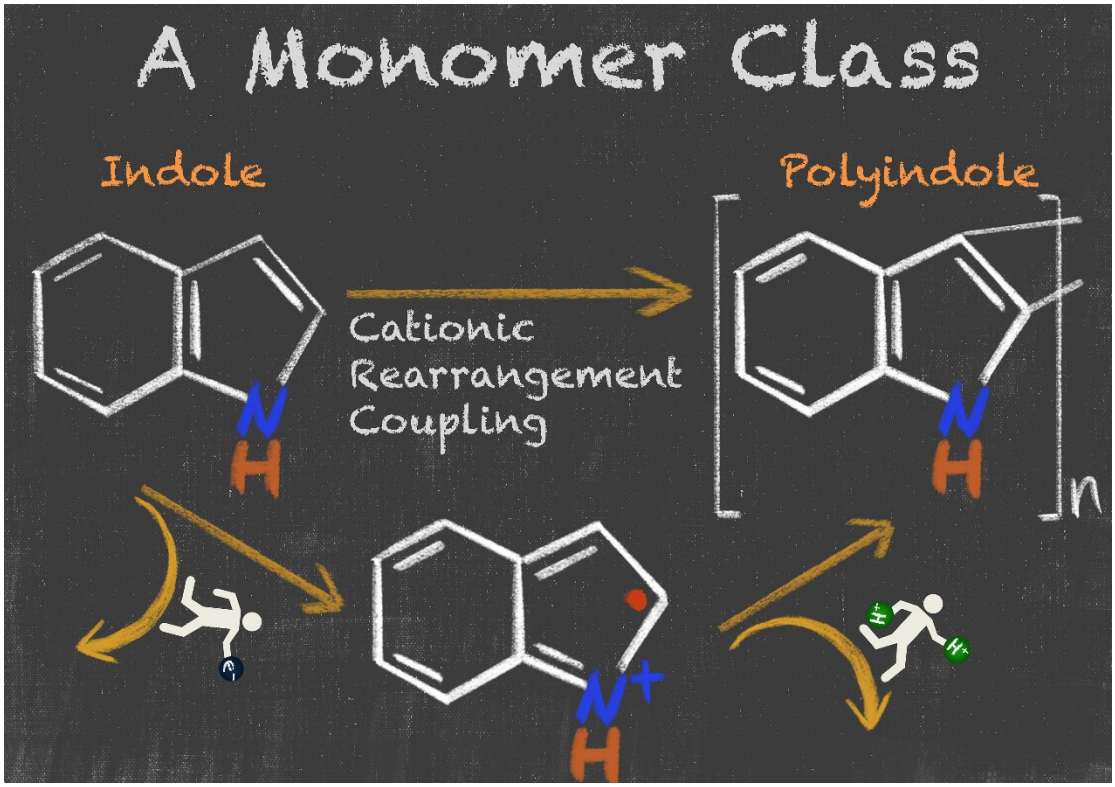

Fig. S1 Schematic diagram of concise version of the mechanism of oxidative polymerization of indole monomers.

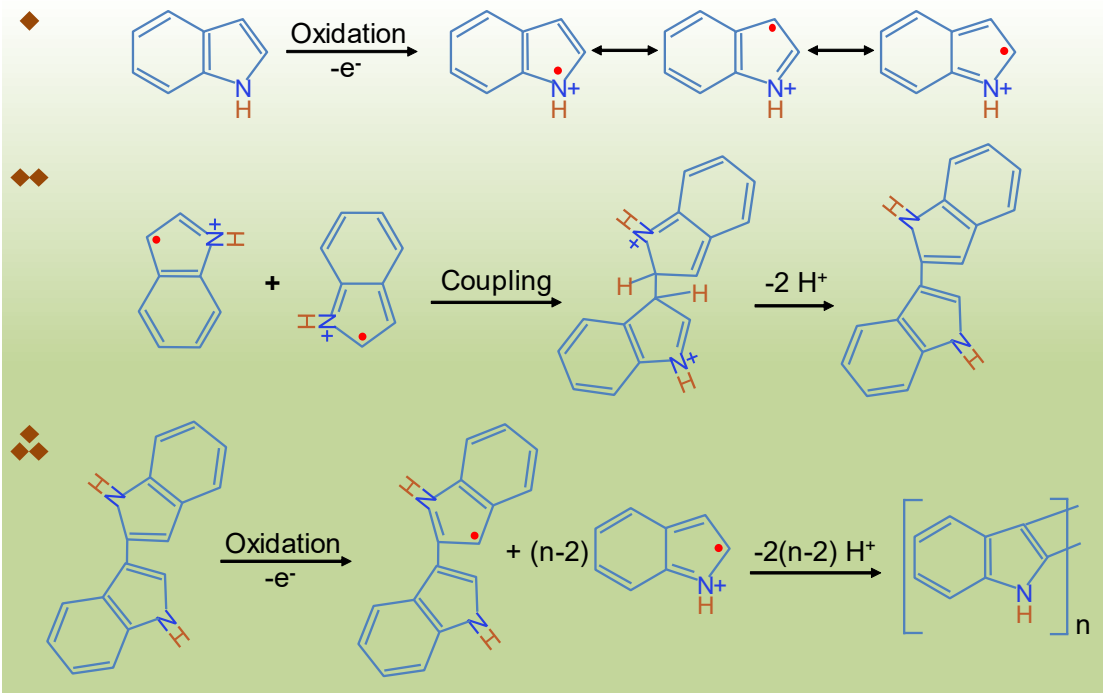

Fig. S2 Schematic diagram of exhaustive version of the mechanism of oxidative polymerization of indole monomers.

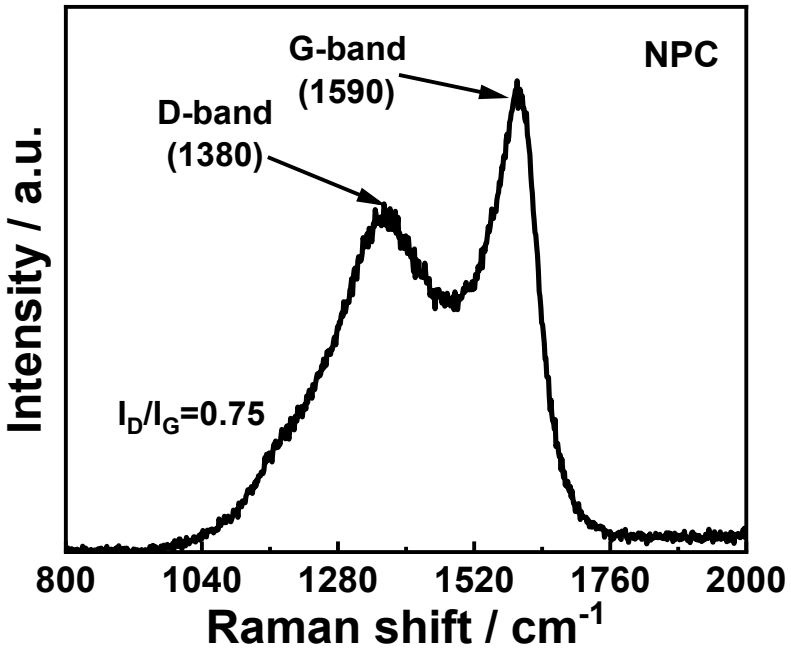

Fig. S3 Raman spectrum of NPC.

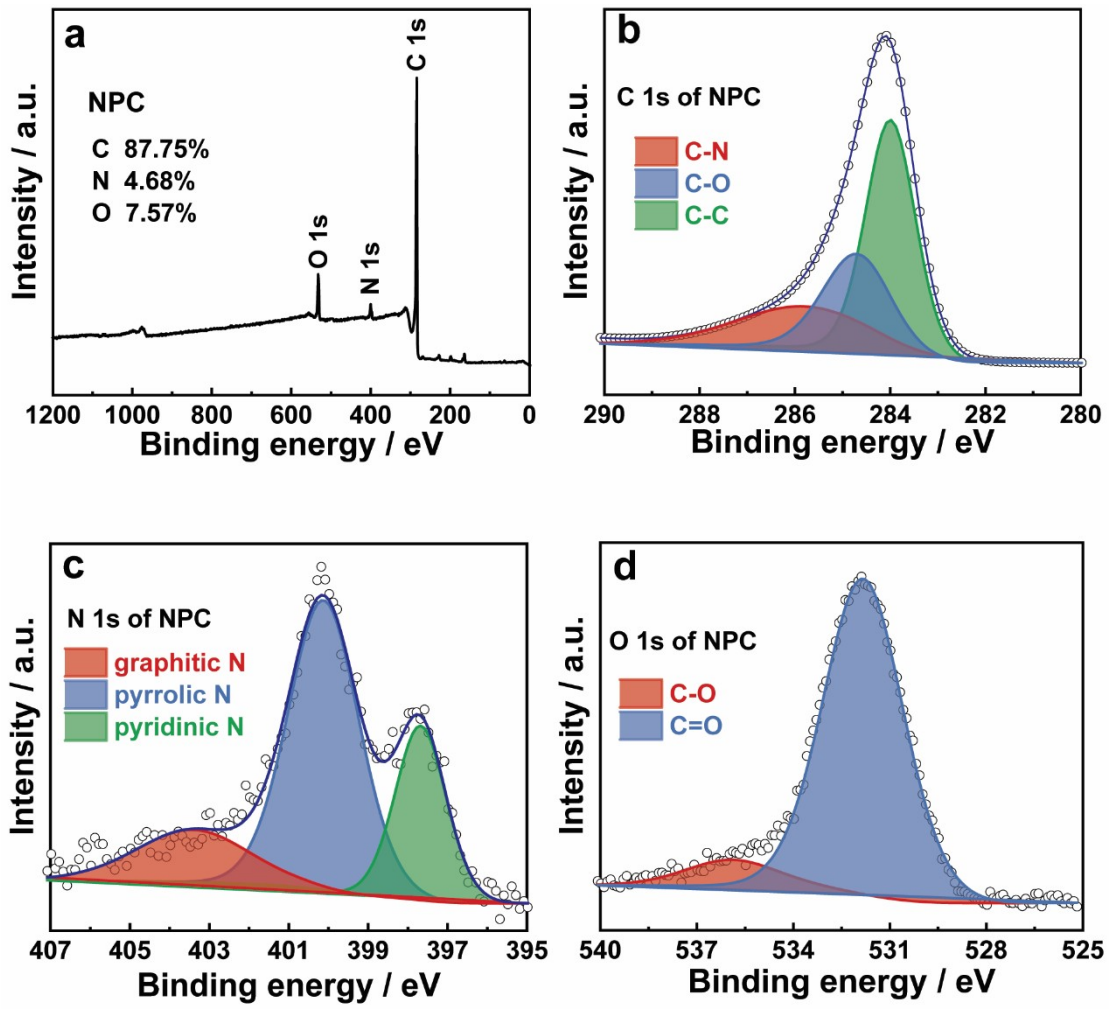

Fig. S4 XPS survey spectrum (a) of NPC; high resolution XPS spectra (b ~ d) of C 1s, N 1s and O 1s, respectively.

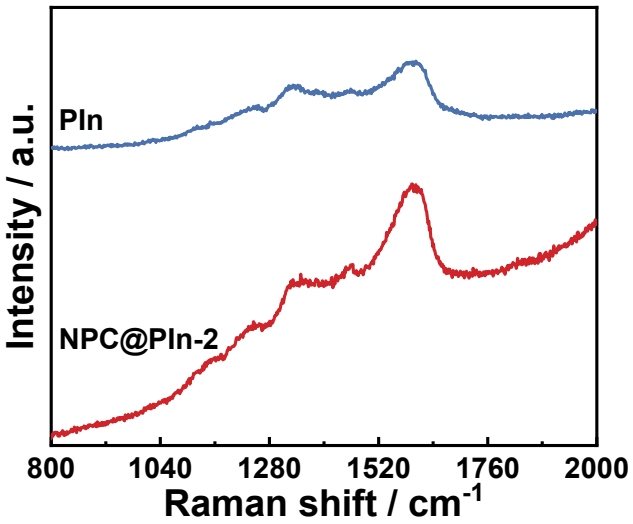

Fig. S5 Raman spectra of PIn and NPC@PIn-2 composite.

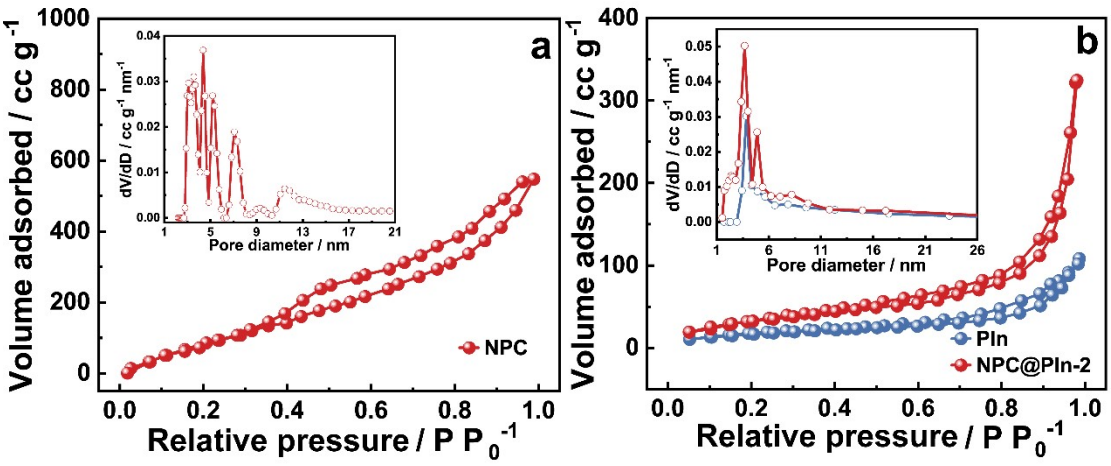

Fig. S6 nitrogen adsorption-desorption isotherms (a) of NPC (insert is the corresponding pore size distribution plot), nitrogen adsorption-desorption isotherms (b) of PIn and NPC@PIn-2 (insert is the corresponding pore size distribution plots).

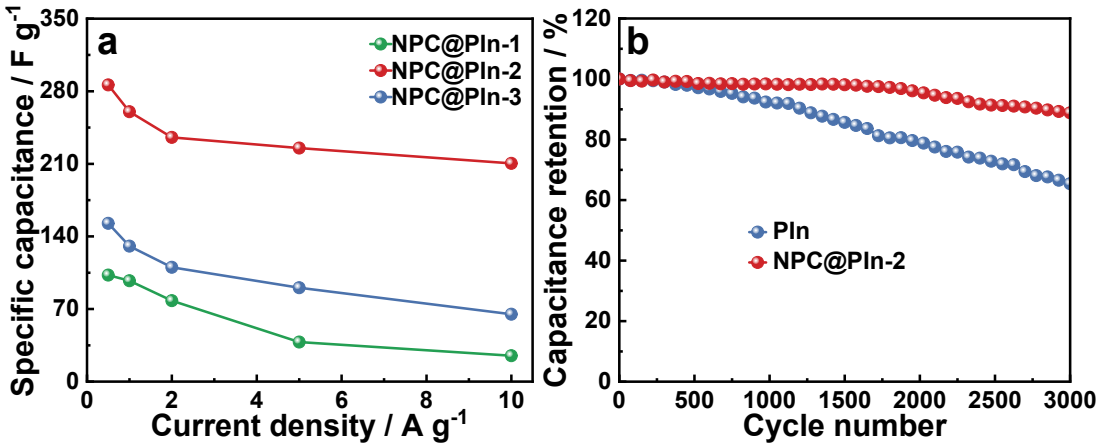

Fig. S7 Rate capabilities (a) of NPC@PIn composites; cyclic stabilities (b) of PIn and NPC@PIn-2 composite at current density of 5 A g^{-1}.

Preparation of $Ti_3C_2T_x$ MXene

$Ti_3C_2T_x$ MXene was prepared by selectively etching Al from Ti_3AlC_2 powder. Briefly, 1.0 g of Ti_3AlC_2 (400 mesh) was slowly added to 20 mL of diluted HF solution (10%) in a Teflon autoclave and kept at 400 rpm min^{-1} for 48 h at room temperature. After etching was complete, the resultant slurry was collected through repeatedly washing and centrifuging until the pH reached approximately neutral. Finally, the product was collected by filtration and dried under vacuum.

Physicochemical characterization of $Ti_3C_2T_x$ MXene

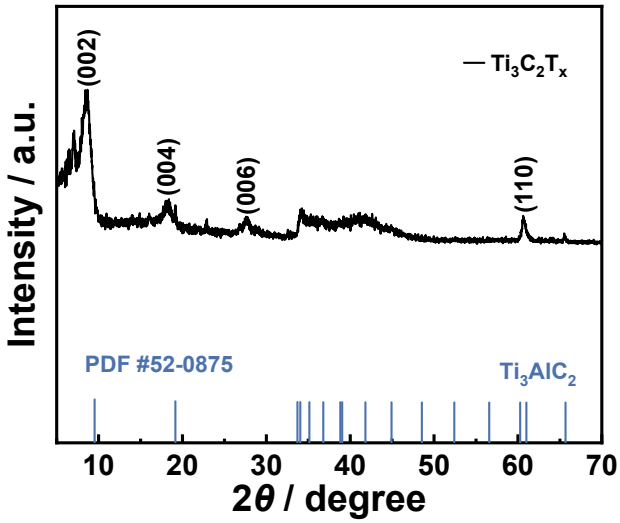

Fig. S8 XRD pattern of $Ti_3C_2T_x$ MXene.

The structure of $Ti_3C_2T_x$ MXene sample is analyzed using X-ray diffraction. As shown in Fig. S8, the typical (002) diffraction peak for $Ti_3C_2T_x$ MXene appears at a 2θ value of 8.4°, while the (002) crystal plane of Ti_3AlC_2 phase is at 9.5°. The shift of (002) peak to a lower angle compared to Ti_3AlC_2 phase confirms the substitution of Al by -F or -OH group[1,2]. Furthermore, the complete disappearance of (104) diffraction peak at 2θ value of 39° for $Ti_3C_2T_x$ MXene sample indicates that Ti_3AlC_2 is entirely converted to $Ti_3C_2T_x$ MXene[3].

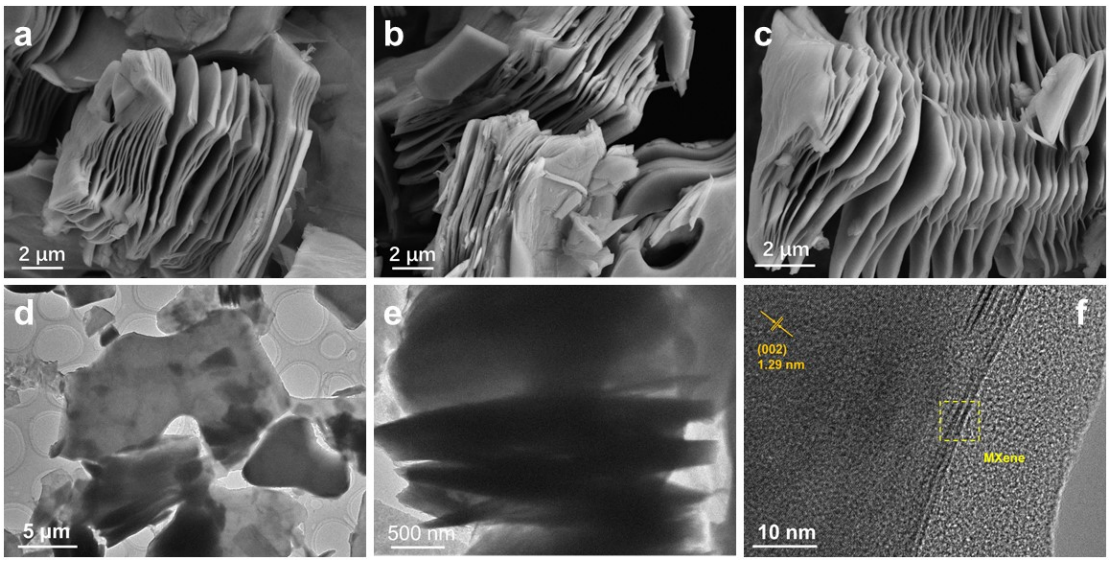

Fig. S9 SEM images (a ~ c) of $Ti_3C_2T_x$ MXene; TEM images (d ~ e) of $Ti_3C_2T_x$ MXene and high-resolution TEM image (f) of $Ti_3C_2T_x$ MXene.

Morphological and microstructural properties of $Ti_3C_2T_x$ MXene are investigated by field emission scanning electron microscopy (FE-SEM) and transmission electron microscopy (TEM) technique. As shown in Fig. S9a ~ S9c, SEM images of $Ti_3C_2T_x$ MXene show a well-aligned, layed structure. TEM images (Fig. S9d ~ S9e) reveal that MXene has a sheet-like structure, confirming its 2D nature that is suitable for supercapacitors because it provides sufficient interspace for ion penetration. The observed inter planar distance of 1.29 nm (Fig. S9f) correspond to (002) plane of MXene. Typically, the 2D layered structure of MXene with excellent electrical conductivity is quite suitable for energy-oriented applications because it offers large electroactive sites and facilitates rapid charge transportation.

References:

[1] W. Sun, Y. Zhao, X. Cheng, J. He and J. Lu, *ACS Appl. Mater. Interfaces*, 2020, **12**, 9865-9871.

[2] P. Yasaei, Q. Tu, Y. Xu, L. Verger, J. Wu, M. Barsoum, G. Shekhawat and V. Dravid, *ACS Nano*, 2019, **13**, 3301-3309.

[3] J. Luo, W. Zhang, H. Yuan, C. Jin, L. Zhang, H. Huang, C. Liang, Y. Xia, J. Zhang, Y. Gan and X. Tao, *ACS Nano*, 2017, **11**, 2459-2469.